Molecular Crystals and Liquid Crystals Science and Technology. Section A. Molecular Crystals and Liquid Crystals
Publication details, including instructions for authors and subscription information:
http://www.tandfonline.com/loi/gmcl19

Thermodynamic Characterization of the Plastic Crystal and Non-Plastic Crystal Phases of C_{70}

Y. Jin [a b], A. Xenopoulos [a b], J. Cheng [a b], W. Chen [a b], B. Wunderlich [a b], M. Diack [a b], C. Jin [a b], R. L. Hettich [a b], R. N. Compton [a b] & G. Guiochon [a b]

[a] Chemistry Division, Oak Ridge National Laboratory, Oak Ridge, Tennessee, 37831-6197

[b] Department of Chemistry, The University of Tennessee, Knoxville, Tennessee, 37996-1600

Version of record first published: 23 Sep 2006.

To cite this article: Y. Jin , A. Xenopoulos , J. Cheng , W. Chen , B. Wunderlich , M. Diack , C. Jin , R. L. Hettich , R. N. Compton & G. Guiochon (1994): Thermodynamic Characterization of the Plastic Crystal and Non-Plastic Crystal Phases of C_{70} , Molecular Crystals and Liquid Crystals Science and Technology. Section A. Molecular Crystals and Liquid Crystals, 257:1, 235-250

To link to this article: http://dx.doi.org/10.1080/10587259408033780

Mol. Cryst. Liq. Cryst., 1994, Vol. 257, pp. 235–250
Reprints available directly from the publisher
Photocopying permitted by license only

Thermodynamic Characterization of the Plastic Crystal and Non-Plastic Crystal Phases of C_{70}

Y. JIN, A. XENOPOULOS, J. CHENG, W. CHEN, B. WUNDERLICH,* M. DIACK, C. JIN, R. L. HETTICH, R. N. COMPTON and G. GUIOCHON

Chemistry Division, Oak Ridge National Laboratory, Oak Ridge, Tennessee 37831-6197 and Department of Chemistry, The University of Tennessee, Knoxville, Tennessee 37996-1600

(Received June 11, 1993; in final form October 12, 1993)

Heat capacity measurements were performed on chromatographically purified C_{70} from 120 to 560 K by DSC. The experimental values were linked to the vibrational heat capacity, calculated based on normal-mode vibration frequencies available from the literature. Good agreement is found, as prior for C_{60}. Major orientational disorder is introduced in two closely spaced transitions, reflecting the change to the phase that displays anisotropic rotation of the rugby-ball shaped molecules. The total entropy of the disordering transitions is 22.4 J/(K mol), slightly lower than that of C_{60}, but additional entropy is gradually acquired between 120 K and the transition temperature, making the total entropy gain higher than that of C_{60}, as expected for a less symmetric molecule. The Debye temperature for the six lattice vibrations of C_{70} was calculated to be 45 K, compared to 53 K for C_{60}. No melting temperature could be detected for C_{70} up to 950 K, but the entropy of fusion is estimated to be 12 J/(K mol). Enthalpies, Gibbs energies, and entropies have been calculated from 0 to 1000 K

Keywords: Fullerene C_{70}, crystal, plastic crystal, orientational disorder, thermodynamic characterization, heat capacity

1. INTRODUCTION

Recent research on fullerene materials has focused on carbon clusters of a size larger than C_{60}. The molecules of C_{70}, with a "rugby-ball" structure, have been the first to become available in quantities allowing macroscopic experimental investigations. Following our previous work on C_{60},[1] we are presenting here the thermodynamic characterization of C_{70}.

Some prior work has been presented in the literature on thermal and structural characterization of C_{70}. Grivei *et al.* presented low temperature heat capacities based on a relaxation time measurement from 3 to 300 K and qualitative DSC to 450 K.[2] Differential thermal analysis, DSC, on chromatographically purified and sublimed samples showed two reproducible transitions with onset temperatures at 276 K (3.5 ± 0.5 J/g) and 337 K (2.7 ± 0.3 J/g).[3] The total ΔH was comparable to that found in C_{60}, indicating possibly a similar orientational disordering. The new data of this research yield a combined ΔH of 7.38 J/g and considerable additional gain of entropy

below the transition temperature. The high-temperature crystal form is expected to be a plastic crystal. Vaughan *et al.*[3] found the X-ray pattern at 440 K can, however, only be indexed as a mixture of two different crystal structures, a hexagonal close packed (hcp) and a face-centered cubic (fcc) polymorph, with an estimate of 21% hcp, both are commensurate with the mobility of the motifs in a plastic crystal. Annealing a sample sublimed for 200 hours at 575 K in a sealed capillary reduces the amount of hcp crystals, but does not eliminate them completely. Although the fcc phase appears to be the equilibrium state above room temperature, the hcp phase is energetically similar to fcc and is easily nucleated so that a prolonged annealing is needed to produce large amount of fcc.

Retention of solvent by C_{70} on crystallization from solution occurs to a much larger extent than for C_{60}. The sharp endotherms in the range of 395 to 445 K reported for crystals grown from toluene[3] are attributed to decomposition of a toluene-C_{70} complex, $C_{70}\cdot C_6H_5CH_3$. The endotherms were not observed upon reheating if the experiment is done in an open pan, but persist after cycling in a sealed pan, indicating that the toluene leaves and reenters the sample on temperature cycling.[4]

The study of large, pure crystals of C_{70} (grown from the vapor phase in a quartz tube under a temperature gradient) by X-ray diffraction and TEM showed that the hexagonal phase is not simply a result of solvent nucleation.[5] Five different polymorphs were identified by cooling and heating crystals grown under such conditions. At low temperature, C_{70} is monoclinic. The low-temperature, monoclinic phase is analyzed in this research by heat capacity measurement. Above the disordering transitions the various other polymorphs are expected not to have noticeably different heat capacities and also their heats of transition are expected to be sufficiently small not to increase the uncertainty introduced by the pretransition heat-capacity increase.

Calculations of the energetics of fullerenes, show that the optimal interaction between C_{70} molecules is, as expected, when the long axes are parallel. The computed cohesive energies of 184 and 207 kJ/mol for C_{60} and C_{70},[5] respectively, are in line with experimentally determined heats of sublimation ($\Delta H_{707K} = 168 \pm 5$ kJ/mol for C_{60} and $\Delta H_{739K} = 180 \pm 9$ kJ/mol for C_{70}).

Two orientational disordering transitions are also indicated in constant-pressure molecular dynamics simulations. Cooling of the high-temperature fcc phase (I) produces an intermediate phase II, with the five-fold axes oriented at 18° with respect to the unique $\langle 111 \rangle$ directions. The motion consists of rotations about the five-fold axis and 120° precessional jumps, resulting in a trigonal symmetry. In the fully ordered phase III, half of the molecules align along $\langle 111 \rangle$ and half along $\langle 110 \rangle$, so that a monoclinic symmetry is obtained.[6]

Various energy-minimizations of the chemical structures were carried out for C_{60} and C_{70}.[8] Eight different bond lengths and 12 different bond angles are reported for C_{70}. The molecule C_{70} was computed to have less torsional strain than C_{60}. Molecular mechanics computations give heats of formation as 2.17 and 2.44 MJ/mol for C_{60} and C_{70}, respectively.[7]

The molecule C_{70} belongs to the symmetry group D_{5h} and should have 31 IR- and 53 Raman-active modes. Both experimental results (Raman and infrared),[8-10] and theoretical studies (using the quantum-chemical method AM1,[12] the QCFF/PI method,[13]

a semiempirical MNDO method,[14] and a modified MOPAC algorithm,[15]) of the vibrational spectra are available. In the most recent experimental study,[11] up to 13 infrared and 33 Raman modes were identified. The agreement of the theoretical studies with experiment is quite good. We used these vibrational analyses to calculate the vibrational heat capacity and compare it with experiment. Combined with the transition data, a complete thermal characterization of C_{70} is possible.

EXPERIMENTAL

Sample

The sample of C_{70} used in this research was obtained from soot prepared using the contact-arc technique described elsewhere.[16,17] It is obtained by evaporating graphite rods (Poco graphite) using a contact-arc discharge (80 A at 40 V), in a helium atmosphere (27 kPa). The fullerenes were extracted from the soot using boiling toluene and the resulting extract was rotary-evaporated and dried under vacuum (until a constant weight was obtained). The purification of the fullerenes C_{60} and C_{70} was realized using a dual column of silica/alumina in a gravity mode with a mixture of hexane/toluene (95:5% v/v) as mobile phase.[18] The purity of the fractions was 98%, estimated using analytical high pressure liquid chromatograph (HPLC) on an octadecyl silane (ODS) chemically bonded phase. Both NMR and mass spectra show no signal of C_{60} present in the sample. The as-received sample was heated up to 473 K in the DSC cell to remove the toluene. The weight loss is about 10%, accounting for the decomposition of the $C_{70} \cdot C_6H_5CH_3$ complex, to be described in more detail in Reference 4.

Calorimetry A commercial Thermal Analyst 2100 system from TA Instruments Inc. with a 912 dual sample DSC and DSC auto-sampler was used for heat capacity measurement and transition analysis. Details about the equipment, operation and software development were given in previous publications.[18–21] A single-run heat capacity measurement technique was developed.[22] Heat capacities were determined from 120 to 560 K with three sets of experiments (120–320 K, 220–460 K, and 320–560 K). Each run was repeated at least three times and the collected data were averaged and smoothed. The error is estimated to be $< 2\%$ above 300 K and $< 5\%$ below 200 K and $< 4\%$ between 200 and 300 K.

All heat capacities were measured at 10 K/min or 5 K/min heating rate with a N_2 gas flow of 10 mL/min above 300 K, and with stationary N_2 gas below 300 K. Heat capacities were calibrated with a sapphire standard. The temperature calibration was carried out using the onsets of the transition peaks for cycloheptane (134.8 and 265.1 K), 1-chlorobutane (150.1 K), cyclohexane (186.1 and 279.7 K), naphthalene (353.42 K), benzoic acid (396.55 K), indium (429.75 K), tin (505.05 K), and potassium nitrate (607.15 K). Sample masses were 5–10 mg. All sample placement was done with the Autosampler for increased repeatability. No weight loss was observed over the temperature range of heat capacity analysis for the C_{70} obtained from the $C_{70} \cdot C_6H_5CH_3$ complex, as described above. The preliminary check for a melting temperature was carried out at 50 K/min heating rate in a qualitative mode. The sample was enclosed for this experiment in a non-hermetically sealed copper pan. No melting temperature could be

detected up to 950 K, the temperature limit of our calorimeter. The weight loss after this experiment, presumably through sublimation, was less than 3%.

In addition to the just described standard calorimetry, a Thermal Analyst 2190 system from TA Instruments Inc. with a prototype modulated DSC (MDSC) was uscd at different heating and cooling rates to determine transitions and heat capacities. The MDSC is an extension to conventional DSC and provides information about reversing and non-reversing characteristics of thermal events. It is able to measure heat capacity at low heating/cooling rate (< 5 K/min) and even at almost isothermal condition. In MDSC, the same heat flux DSC cell is used, but a different temperature (heating/cooling) profile is applied to the sample and reference via the furnace. Specifically, a sinusoidal ripple (modulation) is overlaid on the standard linear temperature ramp. As a result, there are three heating-related experimental variables which can be used to improve DSC results and gain additional information. These variables are heating rate, amplitude of modulation, and frequency or period of modulation. Here we use the amplitude of 0.5 K, period of 60 s/cycle (0.017 Hz), and heating/cooling rates of 1, 5, and 10 K/min respectively. The details and quantitative evaluation of the technique will be discussed in the near future.[24]

Calculation of the Heat Capacity The calculation of heat capacity of polymeric solids from vibrational spectra is well documented in several publications from our laboratory.[25–28] For the case of C_{70}, the heat capacity at constant volume (C_v) is calculated based on a separation of the vibrational spectrum into the internal vibration of the separated molecules and the lattice vibrations, as was done prior for C_{60}.[1] In short, the heat capacity contributions of the 204 vibrations characteristic of the isolated C_{70} molecule are computed from frequencies obtained by normal mode analyses fitted to IR and Raman data. After subtracting these contributions from the experimental C_v, the remaining heat capacity is due to the lattice vibrations and is fitted to a three-dimensional Debye function for 6 degrees of freedom. The fitting parameter is the characteristic Debye temperature Θ_3. Reversing the process, Θ_3 and the table of molecule vibrations permits the computation of the heat capacity due to the vibrational spectrum over a wide temperature range.

For each of the molecule vibrations, we use an Einstein function, $E(\Theta_i)$, to compute the heat capacity contribution, so that the total group vibration contribution is:

$$C_v = R\sum_{i=1}^{N} E(\Theta_i) = R\sum_{i=1}^{N} \frac{(\Theta_i/T)^2 e^{\Theta_i/T}}{(e^{\Theta_i/T}-1)^2} \tag{1}$$

where N is number of vibrational modes, R is the gas constant 8.31454 J/(K mol), T is the temperature in K, and $\Theta_i = h\nu_i/k$ is the characteristic frequency, also expressed in K, (a frequency, ν_i, given in wave numbers, cm^{-1}, as customary spectroscopy, must be multiplied by 1.4388 cm K to yield the frequency in K).

The lattice vibrations are approximated by the three-dimensional Debye function:

$$C_v/NR = D_3(\Theta_3/T) = 3(T/\Theta_3)^3 \int_0^{(\Theta_3/T)} \frac{(\Theta/T)^4 \exp(\Theta/T)}{[\exp(\Theta/T)-1]^2} d(\Theta/T) \tag{2}$$

where T represents, as usual, the temperature in kelvin; R is the gas constant; N, the number of vibrations considered by the equation (for C_{60} and C_{70}, $N = 6$); and Θ_3, the Debye-temperature, the upper frequency limits of the intermolecular frequeny distribution ($1\,\text{Hz} = 8.40 \times 10^{-11}\,\text{K}$). At low temperature Θ_3 can be estimated from:

$$C_v/NR = D_3(\Theta_3/T) = \frac{4\pi^4}{5}(T/\Theta_3)^3 \tag{3}$$

The values of Θ_3 for C_{60} ($\Theta_3 = 53\,\text{K}$) were derived from the experiments of Reference 29 and for C_{70} ($\Theta_3 = 45\,\text{K}$) from Reference 2.

Two sets of molecular normal mode frequencies are reported in the literature[13,15] and were used to calculate the heat capacity contributions for C_{70}:

$$C_{v,\text{molecule}} = \sum_{j=1}^{122} g_j E(\Theta_j) \tag{4}$$

where $E(\Theta_i)$ is the Einstein function and g_j is the degeneracy of vibration j ($\sum g_j = 204$). The frequencies used in the computations are listed in Table I.

The heat capacity at constant volume is then the sum of the two contributions [Equations (1) and (2)]:

$$C_v = C_{v,\text{molecule}} + C_{v,\text{lattice}} \tag{5}$$

The conversion of heat capacity at constant volume to that at constant pressure, C_p, is done by a modified Nernst–Lindemann equation:[30]

$$C_p - C_v = 3RA_0C_pT/T_m^\circ \tag{6}$$

where R is the gas constant; A_0 is a constant, either fitted to experimental data on compressibility and expansivity or approximated by the universal value of 3.9×10^{-3} (K mol)/J and T_m° represents an estimate of the equilibrium melting temperature. For C_{70}, the universal value of A_0 needed to be used because no compressibility and expansivity data are available and T_m° was estimated to be 1500 K,[31] but note that $C_p - C_v$ is a minor correction only, particularly at temperatures below 400 K.

Once the heat capacity is established, the enthalpy (H), entropy (S) and Gibbs function (G) can be easily calculated as follows:

$$H = H^0 + \int_0^{T_d} C_p(T)\,dT + \Delta H_d + \int_{T_d}^{T} C_p(T)\,dT \tag{7}$$

$$S = \int_0^{T_d} \frac{C_p(T)}{T}\,dT + \Delta S_d + \int_{T_d}^{T} \frac{C_p(T)}{T}\,dT \tag{8}$$

$$G = H - TS \tag{9}$$

where ΔH_d and ΔS_d are the enthalpy and entropy of disordering at the equilibrium transition temperature T_d, and H^0 is the enthalpy at absolute zero. The crystal at

TABLE I

Normal-Mode Vibration Frequencies for C_{70}

No. (j)	Group label	Frequency (ν_j), cm^{-1}			Degeneracy (g_j)
		Ref. 13	Ref. 15	expt	
1	A_1'	1633	1831	1568	1
2		1465	1748		1
3		1383	1694		1
4		1220	1452	1232	1
5		1187	1401	1185	1
6		1085	1259	1062	1
7		732	865		1
8		682	761		1
9		570	602	571	1
10		474	571		1
11		404	407		1
12		251	262	260	1
13	A_2'	1532	1639		1
14		1452	1497		1
15		1298	1375		1
16		1146	968		1
17		859	927		1
18		828	791		1
19		653	694		1
20		568	569		1
21		484	499		1
22	A_1''	1658	1761		1
23		1454	1512		1
24		1342	1377		1
25		1041	922		1
26		899	856		1
27		774	810		1
28		772	649		1
29		544	561		1
30		335	334		1
31	A_2''	1565	1835		1
32		1389	1721		1
33		1270	1495		1
34		1217	1346		1
35		1168	1267		1
36		895	1042		1
37		684	759		1
38		592	717		1
39		485	475		1
40		326	332		1
41	E_1'	1640	1813		2
42		1568	1737		2
43		1499	1663		2
44		1424	1615		2
45		1383	1502		2
46		1369	1465		2
47		1245	1430		2
48		1200	1361		2
49		1118	1278		2
50		961	1070		2
51		931	923		2
52		819	871		2
53		748	828		2
54		711	725		2
55		650	678		2
56		585	663		2
57		560	613		2
58		498	517		2

TABLE I (*Continued*)

No. (j)	Group label	Frequency (ν_j), cm^{-1}			Degeneracy (g_j)
		Ref. 13	Ref. 15	expt	
59		412	422		2
60		361	369		2
61		327	334		2
62	E'_2	1645	1804		2
63		1583	1750		2
64		1526	1730	1513	2
65		1463	1590		2
66		1433	1528		2
67		1332	1506		2
68		1265	1414		2
69		1212	1357		2
70		1064	1222		2
71		966	1130		2
72		868	914		2
73		822	896		2
74		781	868		2
75		773	822		2
76		756	801		2
77		722	743		2
78		667	697		2
79		570	554		2
80		501	513		2
81		425	438		2
82		305	307		2
83		216	224		2
84	E''_1	1647	1816		2
85		1592	1737		2
86		1461	1673		2
87		1440	1536		2
88		1360	1460		2
89		1317	1434		2
90		1232	1360		2
91		1186	1335		2
92		1069	1199		2
93		909	897		2
94		806	862		2
95		766	830		2
96		753	784		2
97		699	715		2
98		559	572		2
99		538	538		2
100		489	495		2
101		419	410		2
102		243	252		2
103	E''_2	1642	1801		2
104		1551	1738		2
105		1531	1692		2
106		1460	1585		2
107		1418	1485		2
108		1358	1450		2
109		1245	1402		2
110		1141	1302		2
111		1107	1257		2
112		939	1092		2
113		867	905		2
114		819	810		2
115		739	792		2

TABLE I (*Continued*)

No. (j)	Group label	Frequency (ν_j), cm^{-1} Ref. 13	Ref. 15	expt	Degeneracy (g_j)
116		710	758		2
117		682	663		2
118		610	586		2
119		515	526		2
120		405	415		2
121		391	387		2
122		314	317		2
				Total	204

absolute zero is assumed to be sufficiently perfect to use the third-law entropy of zero in Equation (8).

RESULTS

Heat Capacity of C_{70}

Based on the low temperature heat capacity measured by the relaxation-time method, the heat capacity of C_{70} below 8 K shows a T^3 fit as follow (Figure 4 of Reference 2):

$$C_v = \alpha T^3 \tag{10}$$

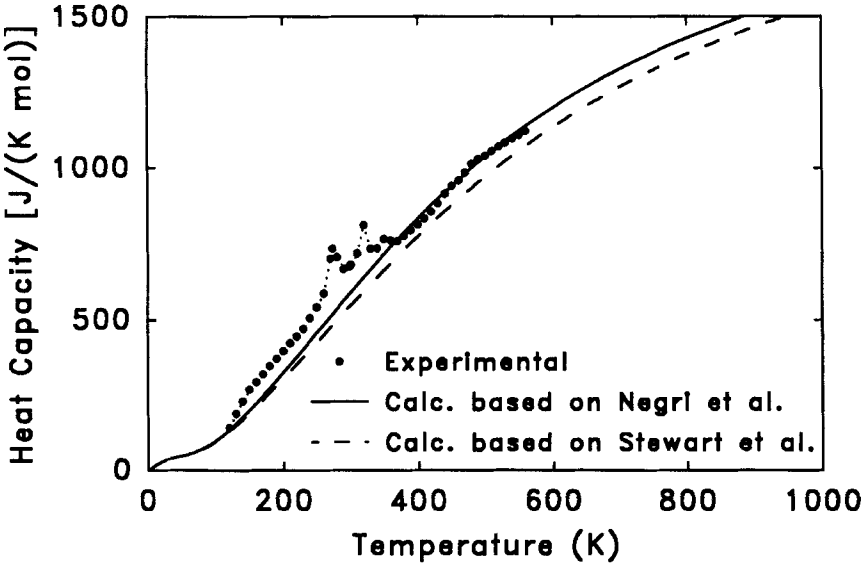

FIGURE 1 Measured heat capacities of C_{70} compared to the calculated heat capacities based on $\Theta_3 = 44.6$ K and the 204 group vibrations of Table I (continuous curve Reference 13, dashed auve, Reference 15).

TABLE II

Calculated and Experimental Heat Capacities of C_{70}

	Heat capacity, J/(K mol)			Deviation, %	
T(K)	expt	calcd[a]	calcd[b]	dev[a]	dev[b]
120.00	141.2	135.5	130.1	−4.2	−8.5
130.00	188.2	155.6	149.0	−20.9	−26.4
140.00	229.5	177.2	169.0	−29.5	−35.8
150.00	268.3	199.9	190.2	−34.2	−41.1
160.00	292.9	223.6	212.1	−31.0	−38.1
170.00	319.8	248.2	234.8	−28.9	−36.2
180.00	346.7	273.3	258.0	−26.8	−34.3
190.00	371.0	299.0	281.7	−24.1	−31.7
200.00	396.2	325.1	305.7	−21.8	−29.6
210.00	423.3	351.6	329.9	−20.4	−28.3
220.00	444.6	378.2	354.3	−17.6	−25.5
230.00	470.6	404.9	378.7	−16.2	−24.3
240.00	506.6	431.7	403.2	−17.4	−25.7
250.00	542.7	458.5	427.6	−18.4	−26.9
260.00	587.6	485.2	452.0	−21.1	−30.0
270.00	700.9	511.8	476.3	−36.9	−47.1
273.15	733.2	520.2	484.0	−41.0	−51.5
280.00	706.4	538.3	500.5	−31.2	−41.1
290.00	667.4	564.6	524.6	−18.2	−27.2
298.15	675.7	585.9	544.1	−15.3	−24.2
300.00	680.2	590.7	548.5	−15.1	−24.0
310.00	719.3	616.5	572.2	−16.7	−25.7
320.00	810.2	642.1	595.7	−26.2	−36.0
330.00	733.9	667.4	618.9	−10.0	−18.6
340.00	735.1	692.3	642.0	−6.2	−14.5
350.00	764.7	716.9	664.8	−6.7	−15.0
360.00	760.9	741.1	687.3	−2.7	−10.7
370.00	758.7	765.0	709.6	0.8	−6.9
380.00	776.1	788.5	731.6	1.6	−6.1
390.00	793.4	811.5	753.4	2.2	−5.3
400.00	813.0	834.2	774.8	2.5	−4.9
410.00	833.0	856.5	795.9	2.7	−4.7
420.00	854.8	878.3	816.7	2.7	−4.7
430.00	882.5	899.7	837.2	1.9	−5.4
440.00	913.9	920.6	857.3	0.7	−6.6
450.00	940.5	941.2	877.2	0.1	−7.2
460.00	958.5	961.3	896.7	0.3	−6.9
470.00	983.7	981.0	915.8	−0.3	−7.4
480.00	1012.2	1000.2	934.7	−1.2	−8.3
490.00	1027.9	1019.0	953.1	−0.9	−7.8
500.00	1040.4	1037.4	971.3	−0.3	−7.1
510.00	1055.6	1055.4	989.1	0.0	−6.7
520.00	1070.0	1073.0	1006.6	0.3	−6.3
530.00	1082.9	1090.1	1023.7	0.7	−5.8
540.00	1095.8	1106.9	1040.6	1.0	−5.3
550.00	1108.0	1123.3	1057.0	1.4	−4.8
560.00	1120.8	1139.3	1073.2	1.6	−4.4

[a] Calculation based on the frequencies given by Negri *et al.*[13]
[b] Calculation based on the frequencies given by Stewart *et al.*[15]

where $\alpha = 5.2 \times 10^{-5}$ J/(g K^4). Combining with Equation (3) and assuming $N = 6$, one can get a $\Theta_3 = 44.6$ K for C_{70}. With the group vibrations of Table I, one can easily calculate the heat capacity at any temperature. Figure 1 shows experimental and calculated heat capacities of C_{70} for the temperature range from 0 to 1000 K. The numerical data are listed in Table II from 120 to 560 K together with the differences between the experimental and calculated data. Data of both standard DSC and modulated DSC were averaged in the higher temperature range.

Transitions of C_{70}

The samples, when preheated to remove the initially present complex $C_{70} \cdot C_6H_5CH_3$, show three transitions between 250 and 380 K (heating rate of 10 K/min). In addition to the two transitions reported already in the literature[3] we detected a very small, third transition. The temperatures, enthalpies and entropies of the transitions are given in Table III. Further studies were carried out at different heating/cooling rates by

TABLE III

Transition Parameters for C_{70} at 10 K/min Heating Rate.*

T_0(K)	T_p(K)	ΔH(J/g)	ΔS[J/(K mol)]
261	275	4.44	14.3
303	321	2.55	7.1
338	347	0.39	1.0
Total		7.38	22.4

* T_0 = onset of the transition peaks, T_p = peak temperature.

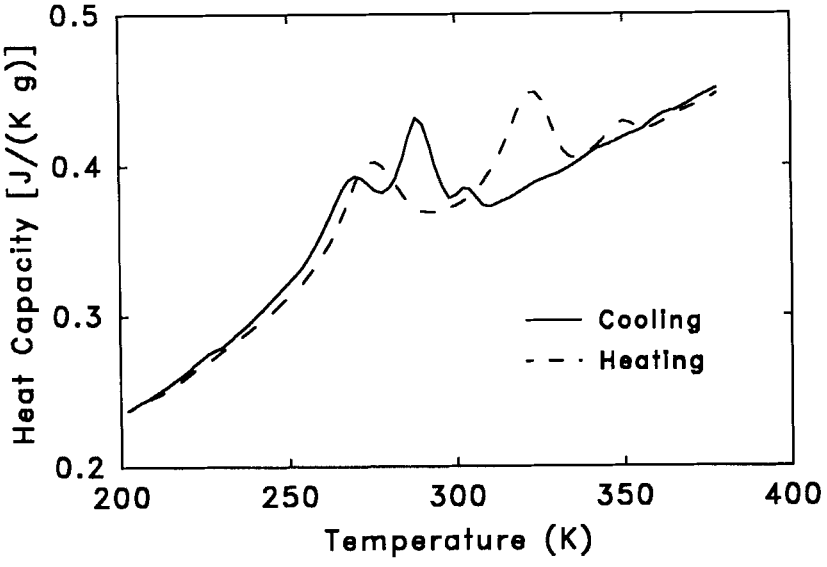

FIGURE 2 Heat capacity of C_{70} at 5 K/min on heating and cooling at a rate of 5 K/min.

TABLE IV

Peak Temperatures for the Transitions of C_{70} at Different Heating/Cooling Rates.*

Heating/cooling rate (K/min)	Heating			Cooling		
1	273	320	345	306	291	272
5	275	321	347	303	288	270
10	276	323	351	301	286	269

* Based on heat capacity measured by modulated DSC.

modulated DSC. Figure 2 shows heat capacity of C_{70} at heating and cooling rate of 5 K/min. The effect of different heating/cooling rates on these disordering transitions are given in Table IV.

After the sample was heated above 600 K, the disorder transitions were not repeatable. To detect any changes in the sample, it was further extracted with hot toluene for 10 hours. Only a small amount of the sample could be brought into solution. Mass spectrometry revealed that *both* extract and residue were still C_{70}, although the extract shows a slightly different disordering transition behavior from the original, toluene precipitated sample. It was suggested by the referee of the paper that these changes may indicate beginning decomposition of dimerized or polymerized C_{70}.

An attempt has also been made to measure the heat capacity of C_{70} in air (without N_2 gas flow). Due to the oxidation of C_{70}, the heat capacity can not be measured under

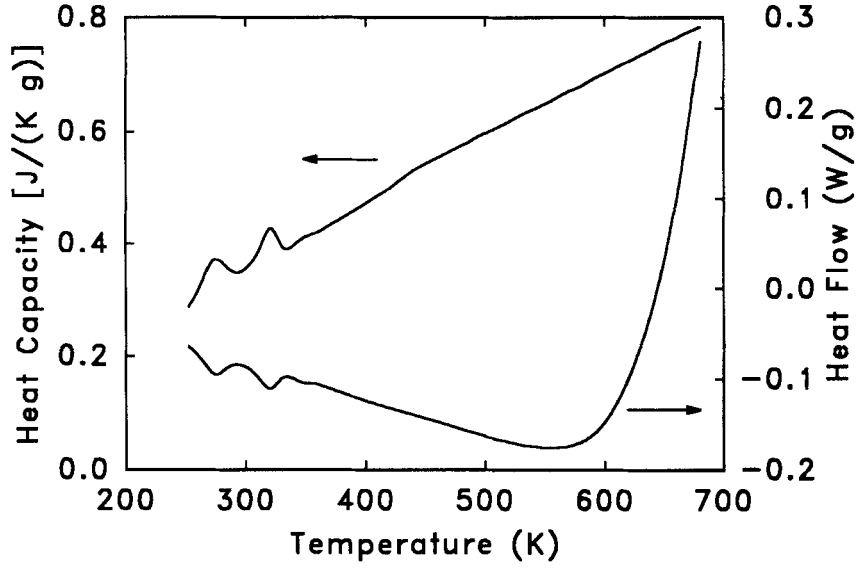

FIGURE 3 Heat capacity (reversing) and heat flow (non-reversing) of C_{70} at higher temperature in air. The oxidation exotherm starts between 500 and 600 K. The small break in the heat capacity between 400 and 500 K is an instrument effect and disappears on point by point calibration with sapphire as done for derivation of the data in Table II.

these conditions by conventional DSC, but since the oxidation is a non-reversing process and involves only very small amount of the sample, it is possible to measured heat capacity by modulated DSC, even in the presence of the strong exotherm, as shown in Figure 3. From the heat-flow curves it can be seen that oxidation starts at about 500 K.

Thermodynamic Functions

The thermodynamic functions H, S, and G have been established based on Equations (7–9) and are shown in Figure 4. Tabular values can be obtained from the authors on request through our *ATHAS* data bank.

DISCUSSION

Heat Capacity of C_{70}

Figure 1 shows that the measured heat capacity of C_{70} agrees above 400 K reasonably well with the calculated C_p based on Reference 13. Below the transition, the experimental heat capacity does not drop to the level of the vibrational heat capacity. This excess heat capacity is an indication of an earlier beginning of orientational disordering and will be discussed below.

It must be mentioned that above 100 K the heat capacity contribution from the lattice vibrations ($6N$) is relatively small and constant, compared to that from the

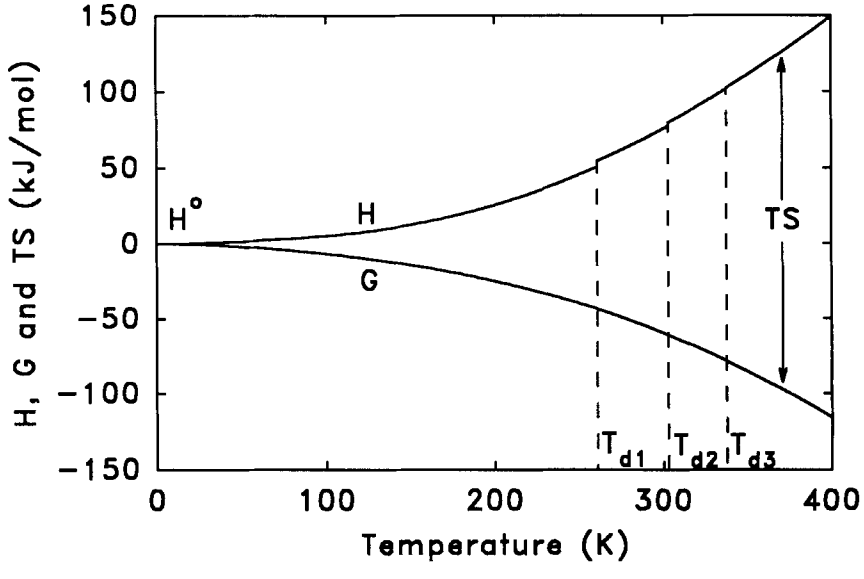

FIGURE 4 Thermodynamic functions (H, S, G) of C_{70} Note that $TS = H - G$.

molecule vibrations [full excitation yields a $6R$ contribution to $C_v \approx 50$ J/(K mol)]. At present, the precision of the heat capcities between 10 and 120 K cannot be considered experimentally verified. The heat capacity of C_{70} reported by Grivei, *et al.*,[2] although reasonable from 3 to 6.5 K (where we used the data to compute Θ_3), becomes extremely high between 10 and 200 K. Their Figure 3 shows, for example, at 120 K a C_p of 420 J/(K mol) which is 200% above the data we report in Table II. Only a systematic error can account for such discrepancies. For this reason only Figures 4 of Reference 13 was accepted for this discussion (data from 3 to 6.5 K).

It also needs to be pointed out that $N = 180$ or 210 used in the literature[13] for the discussion of the low temperature heat capacity of C_{60} and C_{70}, respectively, leads to unreasonable theta-temperatures since the intramolecular vibrations are of much higher frequency. Only six degrees of freedom of motion exist for the lattice vibrations. The lowest Θ_i in Equation (1) is about 300 K, compared to the Θ_3 of 44.6 K for the lattice vibrations.

One expects the value of Θ_3 to be proportional to the ratio of the square root of force constant to mass. The ratio of Θ_3 for C_{60} and C_{70} is 1.18, which suggests stronger intermolecular forces for C_{60}, since the ratio of the square roots of the molecular masses is only 1.08.

Figure 5 gives a comparison of the low temperature heat capacities of C_{60} and C_{70} with diamond and graphite. Clearly, diamond and graphite have none of the low frequency lattice vibrations of the fullerenes that lead to a limiting heat capacity of about 50 J/(K mol) [0.07 J/(K g) for C_{60} and 0.06 J/(K g) for C_{70}]. The lattice vibrations of graphite reflect the weak bonding between the planes of the strongly bonded carbon

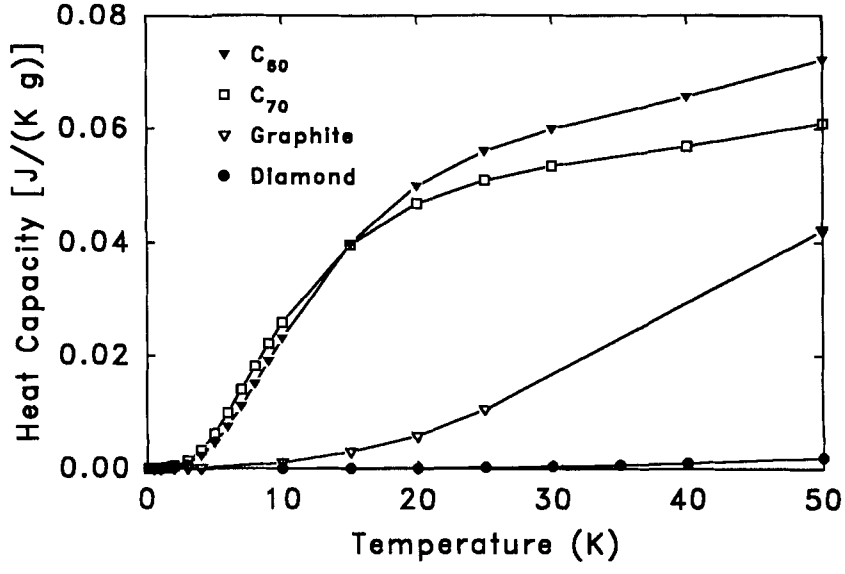

FIGURE 5 Comparison of the low-temperature heat capacities of C_{60}, C_{70}, graphite and diamond. The C_{60} and C_{70} data are calculated based on the discussed group vibrations and Debye temperatures (53 K for C_{60}, 44.6 K for C_{70}).

atoms ($\Theta_3 = 760$ K), while diamond is best described with a Θ_3 of 2050 K, accounting for the uniform sp^3-hybrid bonds.[32] At about 100 K, graphite, C_{60}, and C_{70} have similar heat capacities except for the disordering transitions. Such similarity is expected due to the similarity in intramolecular bonding. Diamond crosses the heat capacity of the fullerenes and graphite at about 1000 K since the sp^3-hybrid bonds, though strong, are somewhat weaker than the sp^2-bonds. Ultimately all carbon allotropes are expected to reach the same specific heat capacity of $3R/12.011$ J/(K g).

Transitions and Large-Amplitude Motion

The heat capacity of Figure 1 shows two major endotherms at around 300 K. The third, small endotherm at slightly higher temperature may be an indication of a higher transition temperature in one of the polymorphs of C_{70}, or even a transition between the polymorphs. The heat capacity below the transition peaks does not match the calculated vibration-only heat capacity above 120 K, an indication that a large amount of disorder may be introduced more gradually at lower temperature. Details of this low-temperature motion will be discussed along with the motion in the C_{70}·toluene complex in the following paper, based on NMR evidence. Adding the additional entropy contained in the higher heat capacity to the entropy of transition would result in an overall entropy of disordering of 70.4 J/(K mol) instead of the 22.4 J/(K mol) of Table III. In light of the greater asymmetry of C_{70} when compared to C_{60} a larger ΔH_d seems reasonable. Typical entropies of transition of asymmetric molecules on gaining rotational freedom in a plastic crystal is 20–50 J/(K mol),[32] i.e., 22.4 is on the low side and 70.4 J/(K mol) would be on the high side. In any case, considering the whole transition range from 120 to 350 K, C_{70} has a higher transition entropy than C_{60}.

The superheating and supercooling of the transitions of C_{70} changes little with heating/cooling rates, as is shown in Table IV. But at the same heating/cooling rate (for example at 5 K/min, as shown in Figure 2), the two higher transition show a supercooling of about 40 K, while the lowest transition supercools by only 5 K. The breadth of the transitions narrows only little on cooling. This observation would be in line with a greater need to order orientationally in the upper transition, connected most likely with a more significant crystal structure change.

Thermodynamic Functions of C_{70}

By knowing the heat capacity of C_{70}, the thermodynamic functions of C_{70} can be easily calculated based on Equations (6–8). The data have been plotted in Figure 4. As mentioned above, tabular values are available through the *ATHAS* data bank. With the knowledge of heat capacity the data shown can easily extrapolated to 1000 K and above. Uncertainties in the thermodynamic functions arise from the multitude of possible crystal structures. The transitions between phases of similar large-amplitude motion are expected to have, however, small heat and entropy changes. The major changes in H, S, and G occur when the large-amplitude motion changes. The pretransition change in order remains also still with a rather large error limit. As soon as more precise transition parameters become available, it is easy to correct the integrations

since the heat capacities are not expected to be altered significantly. Our data bank is updated continuously.

From vapor pressure measurements,[6] the equilibrium entropy of sublimation can be estimated to be 125 J/(K mol). Assuming the entropy of vaporization from the liquid state to be 113 J/(K mol) (Trouton's rule), one can estimate that the entropy of isotropization (ultimate fusion of the plastic crystal) is 12 J/(K mol). This estimate is also in accord with Richards' rule of 7–14 J/(K mol) entropy change for the attainment of positional (translational) disorder. The heat of isotropization could thus be expected to be about 18 kJ/mol assuming the isotropization (melting) temperature is 1500 K.

Oxidation on Heating

The heat flow registered in Figure 3 shows a strong oxidation beyond 500 K This is in perfect agreement with thermogravimetry on C_{70} under similar conditions.[33] In comparison to C_{60}, C_{70} begins to oxidize 100 K earlier (100 K/min).

Acknowledgments

This work was supported by the Division of Materials Research, National Science Foundation, Polymers Program, Grant # DMR 92-00520 and the Division of Materials Sciences, Office of Basic Energy Sciences, U.S. Department of Energy, under Contract DE-AC05-84OR21400 with Martin Marietta Energy Systems, Inc. Part of work was also supported by Grant DE-FG05-88ER13859 from the U.S. Department of Energy, Office of Basic Energy Sciences, and by the cooperative agreement between the University of Tennessee and the Oak Ridge National Laboratory. Thanks are given to TA Instruments, Inc. (New Castle, DE) for providing the modulated DSC equipment and softwares.

References

1. Y. Jin, J. Cheng, M. Varma-Nair, G. Liang, Y. Fu, B. Wunderlich, X. D. Xiang, R. Mostovoy and A. K. Zettl, *J. Phys. Chem.*, **96**, 5151(1992).
2. E. Grivei, B. Nysten, M. Cassart, J.-P. Issi, C. Fabre and A. Rassat, *Phys. Rev. B*, **47**, 47 (1993).
3. G. B. M. Vaughan, P. A. Heiney, J. E. Fisher, D. E. Luzzi, D. A. Ricketts-Foot, A. R. McGhie, Y.-W. Hui, A. L. Smith, D. E. Cox, W. J. Romanow, B. H. Allen, N. Coustel, J. P. McCauley, Jr., and A. B. Smith III, *Science*, **254**, 1350 (1991).
4. J. Cheng, Y. Jin, A. Xenopoulos, W. Chen, B. Wunderlich, M. Diak, C. Jin and R. N. Compton, adjoining paper.
5. M. A. Verheijen, H. Meekes, G. Meijer, P. Bennema, J. L. de Boer, S. van Smaalen, G. van Tendeloo, S. Amelinckx, S. Muto and J. van Landuyt, *Chem. Phys.*, **166**, 287 (1992).
6. Y. Guo, N. Karasawa and W. A. Goddard III, *Nature*, **351**, 464 (1991).
7. M. Sprik, A. Cheng and M. L. Klein, *Phys. Rev. Lett.*, **62**, 1660 (1992).
8. M. Froimowitz, *J. Comput. Chem.*, **12**, 1129 (1991); see also, for example, G. E. Scuseria, *Chem. Phys. Lett.*, **180**, 451 (1991), and J. Baker, P. W. Fowler, P. Lazzeretti, M. Malagoli and R. Zanasi, *Ibid.*, **184**, 182 (1991).
9. D. S. Bethune, G. Meijer, W. C. Tang, H. J. Rosen, W. G. Golden, H. Seki, C. A. Brown and M. S. de Vries, *Chem. Phys. Lett.* **179**, 181 (1991).
10. J. P. Hare, T. J. Dennis, H. W. Kroto, R. Taylor, A. W. Allaf, S. Balm and D. R. M. Walton, *J. Chem. Soc., Chem. Commun.* **66**, 412 (1991).
11. R. Meilunas, R. P. H. Chang, S. Liu, M. Jensen and M. A. Kappes, *J. Appl. Phys.*, **70**, 5128 (1991).
12. Z. Slanina, J. M. Rudziński, M. Togasi, and E. Ōsawa, *J. Mol. Struct. (Theochem)* **202**, 169 (1989).
13. F. Negri, G. Orlandi and F. Zerbetto, *J. Am. Chem. Soc.*, **113**, 6037 (1991).
14. K. Raghavachari and C. M. Rohlfing, *J. Phys. Chem.*, **95**, 5768 (1991).
15. J. J. P. Stewart and M. B. Coolidge, *J. Comput. Chem.*, **12**, 1157 (1991).
16. W. Krätschmer, L. D. Lamb, K Fostiropoulos and D. Huffman, *Nature*, **347**, 354 (1990).

17. M. Diack, R. L. Hettich, R. N. Compton, and G. Guiochon, *Anal. Chem.*, **64**, 2143 (1992).
18. M. Diack, R. N. Compton and G. Guiochon, *J. Chromatogr.* (submitted).
19. Y. Jin and B. Wunderlich, *J. Therm. Anal.*, **36**, 765 (1990).
20. Y. Jin and B. Wunderlich, *J. Therm. Anal.*, **361**, 1519 (1990).
21. Y. Jin and B. Wunderlich, *J. Therm. Anal.*, **38**, 2257 (1992).
22. Y. Jin and B. Wunderlich, *Thermochem. Acta*, **226**, 155 (1993).
23. B. Wunderlich, *J. Therm. Anal.*, **32**, 1949 (1987).
24. Y. Jin, A. Boller and B. Wunderlich, *J. Therm. Anal.*, in press, 1994.
25. Yu. V. Cheban, S.-F. Lau, and B. Wunderlich, *Colloid Polymer Sci.*, **260**, 9 (1982).
26. S.-F. Lau and B. Wunderlich, *J. Thermal Anal.*, **28**, 59 (1983).
27. K. Loufakis and B. Wunderlich, *J. Phys. Chem.*, **92**, 4205 (1988).
28. H. S. Bu, S. Z. D. Cheng and B. Wunderlich, *J. Phys. Chem.*, **91**, 4179 (1987).
29. T. Matsuo, H. Suga, W. I. F. David, R. M. Ibberson, P. Bernier, A. Zahab, C.Fabre, A. Rassat and A. Dworkin, *Solid State Communications*, **83**, 711 (1992).
30. R. Pan, M. Varma-Nair and B. Wunderlich, *J. Therm. Anal.*, **35**, 955 (1989).
31. C. Pan, M. S. Chandrasekharaiah, D. Agan, R. H. Hauge and J. L. Margrave, *J. Phys. Chem.*, **96**, 6752 (1992).
32. B. Wunderlich, *Thermal Analysis*, Academic Press, Boston, 1990.
33. H. G. Wiedemann and G. Bayer, *Thermochim. Acta*, **214**, 85 (1993).